

See discussions, stats, and author profiles for this publication at: <https://www.researchgate.net/publication/26752033>

# Bioinorganic Magnetic Core-Shell Nanocomposites Carrying Antiarthritic Agents: Intercalation of Ibuprofen and Glucuronic Acid into Mg-Al-Layered Double Hydroxides Supported on Magn...

ARTICLE in INORGANIC CHEMISTRY · SEPTEMBER 2009

Impact Factor: 4.76 · DOI: 10.1021/ic901097a · Source: PubMed

---

CITATIONS

38

---

READS

25

4 AUTHORS, INCLUDING:



Ahmet Ay

Hacettepe University

21 PUBLICATIONS 246 CITATIONS

SEE PROFILE



Birgul Zümreoglu-Karan

Hacettepe University

59 PUBLICATIONS 515 CITATIONS

SEE PROFILE

## Bioinorganic Magnetic Core–Shell Nanocomposites Carrying Antiarthritic Agents: Intercalation of Ibuprofen and Glucuronic Acid into Mg–Al–Layered Double Hydroxides Supported on Magnesium Ferrite

Ahmet Nedim Ay,<sup>†</sup> Birgül Zümreoglu-Karan,<sup>\*,†</sup> Abidin Temel,<sup>‡</sup> and Vicente Rives<sup>§</sup>

<sup>†</sup>Hacettepe University, Chemistry Department, Beytepe Campus, 06800 Ankara, Turkey,

<sup>‡</sup>Hacettepe University, Department of Geological Engineering, Beytepe Campus, 06800 Ankara, Turkey, and

<sup>§</sup>GIR-QUESCAT, Departamento de Química Inorganica, Universidad de Salamanca, 37008 Salamanca, Spain

Received June 7, 2009

This paper describes the synthesis and characterization of a composite constituted by an antiarthritic agent (AA) intercalated into a layered double hydroxide (LDH) supported on magnesium ferrite. Core–shell nanocomposites were prepared by depositing Mg–Al–NO<sub>3</sub>–LDH on a MgFe<sub>2</sub>O<sub>4</sub> core prepared by calcination of a nonstoichiometric Mg–Fe–CO<sub>3</sub>–LDH. Intercalation of ibuprofen and glucuronate anions was performed by ion-exchange with nitrate ions. The structural characteristics of the obtained products were investigated by powder X-ray diffraction, element chemical analysis, Fourier transform infrared spectroscopy, and thermogravimetric analysis. Morphologies of the nanocomposite particles were examined by scanning electron microscopy and transmission electron microscopy. The products were shown to intercalate substantial amounts of AA with enhanced thermal stabilities. Room-temperature magnetic measurements by vibrating sample magnetometry revealed that the products show soft ferromagnetic properties suitable for potential utilization in magnetic arthritis therapy.

### Introduction

Layered double hydroxides (LDHs) have recently received considerable attention because of their potential as ion-exchange materials, catalysts, sorbents, antacids, and so forth.<sup>1,2</sup> The general formula of LDHs is [M<sup>II</sup><sub>1-x</sub>M<sup>III</sup><sub>x</sub>(OH)<sub>2</sub>]<sup>x+</sup>[A<sup>n-</sup><sub>x/n</sub>·yH<sub>2</sub>O]<sup>x-</sup>, where M<sup>II</sup> and M<sup>III</sup> are divalent and trivalent metal cations, respectively, and A<sup>n-</sup> is an *n*-valent anion. These compounds have layered crystal structures with wide variations in the nature of the cations and M<sup>II</sup>/M<sup>III</sup> molar ratios, as well as in the type of anions. They qualitatively resemble the conventional intercalation compounds but with complete charge separation between gallery ions and layers. The compositional diversity in the layers and interlayer anions leads to a functional diversity which allows them to be used for a variety of materials applications.

More recently, interest has been focused on using these materials in the health industry as drug supports or matrices.<sup>3–5</sup>

These layered solids have been regarded as inorganic drug carriers due to their ability to intercalate biomolecules, particularly negatively charged ones, between the positively charged layers and then release them on demand. Apart from their potential to deliver drugs in vivo, it will be hopefully possible to control the drug release point and pharmacokinetic profile.

The structures of most of the LDHs correspond to that of the mineral hydrotalcite (HT/Mg<sub>6</sub>Al<sub>2</sub>(OH)<sub>16</sub>CO<sub>3</sub>·4H<sub>2</sub>O). HT-like LDHs are biocompatible<sup>6</sup> and have found pharmaceutical applications as antacids,<sup>7</sup> ingredients in sustained-release pharmaceuticals containing nifedipine,<sup>8</sup> for stabilizing pharmaceutical compositions,<sup>9</sup> and for preparing aluminum magnesium salts of antipyretic, analgesic, and anti-inflammatory drugs.<sup>10</sup> The antacid pharmaceutical property of LDHs<sup>11</sup> makes them effective hosts for the immobilization of nonsteroidal anti-inflammatory drugs (NSAIDs) aiming to reduce gastric irritation side effects. It has been

\*To whom correspondence should be addressed. E-mail: bkaran@hacettepe.edu.tr.

(1) *Layered Double Hydroxides: Present and Future*; Rives, V., Ed.; Science Publishers: New York, 2001.

(2) Duan, X.; Evans, D. G. *Struct. Bonding (Berlin)* **2006**, 119, 193–223.

(3) Choy, J.-H.; Park, M.; Oh, J.-M. *Curr. Nanosci.* **2006**, 2, 275–281.

(4) Choy, J.-H.; Choi, S.-J.; Oh, J.-M.; Park, T. *Appl. Clay Sci.* **2007**, 36, 122–132.

(5) Del Hoyo, C. *Appl. Clay Sci.* **2007**, 36, 103–121.

(6) Cavani, F.; Trifiro, F.; Vaccari, A. *Catal. Today* **1991**, 11, 173–301.

(7) Goodman, L. S.; Gilman, A. *The Pharmacological Basis of Therapeutics*, VI; MacMillan Publishing Co, Inc: New York, 1975.

(8) Doi, N.; Nitta, S.; Kusari, M.; Takahashi, N. *Jpn. Kokai Tokkyo Koho JP 60 255 719*, **1985**.

(9) Ueno, M.; Kubota, H. U.S. Patent 4,666,919, **1987**.

(10) Kyowa Hakko Kogyo Co., *Jpn. Kokai Tokkyo Koho JP 60 10 039*, **1985**.

(11) Serna, C. J.; White, J. L.; Hern, S. L. *J. Pharm. Sci.* **1978**, 67, 324–327.

shown that many common NSAIDs, such as diclofenac,<sup>12,13</sup> ibuprofen (IBU),<sup>12,14–17</sup> indomethacin,<sup>18,19</sup> fenamates<sup>20,21</sup> and naproxen<sup>12,22,23</sup> intercalate, via ion exchange, into HT-like layered double hydroxides. Ambrogi et al.<sup>14</sup> succeeded in producing a LDH compound loaded 50% w/w with ibuprofen by exchanging the chloride ions in the precursor Mg–Al–Cl–LDH. In all of these studies, the thermal stability of the intercalated NSAIDs was reported to be enhanced compared with that of the pure form before intercalation.

The combination of these unique properties of LDHs with magnetic materials has offered a new perspective in drug delivery systems. Zhang et al.<sup>24</sup> synthesized in 2005 a nano-scale magnetic composite by intercalating 5-aminosalicylic acid in Zn–Al–LDH supported on a MgFe<sub>2</sub>O<sub>4</sub> core, which had been prepared by calcination of a Mg–Fe–LDH. The concept of supporting the drug-intercalated LDH on a magnetic core and guiding the material to the targeted site by means of an external magnetic field deeply fascinated chemists following this report. Carja et al. applied this concept to the intercalation of aspirin in Mg–Al–LDH supported on FeO<sub>x</sub>/Fe–LDH.<sup>25</sup> Very recently, Zhang et al.<sup>26</sup> reported the intercalation of diclofenac into Mg–Al–LDH coated on the surface of the magnesium ferrite core. The authors also investigated the in vitro release of the drug with and without a magnetic field and proposed a microstructure-dependent release mechanism. The synthesis of the magnetic spinel core by calcining an iron-containing LDH precursor has been another attraction which affords stoichiometric magnesium ferrite.<sup>27</sup> MgFe<sub>2</sub>O<sub>4</sub> is a soft magnetic material,<sup>28</sup> and drugs intercalated in MgFe<sub>2</sub>O<sub>4</sub>-supported LDHs can be effective alternatives to the conventional magnetic drug carriers<sup>29,30</sup> with superior tailoring properties.

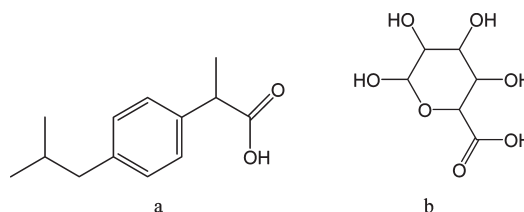


Figure 1. (a) Ibuprofen and (b) glucuronic acid.

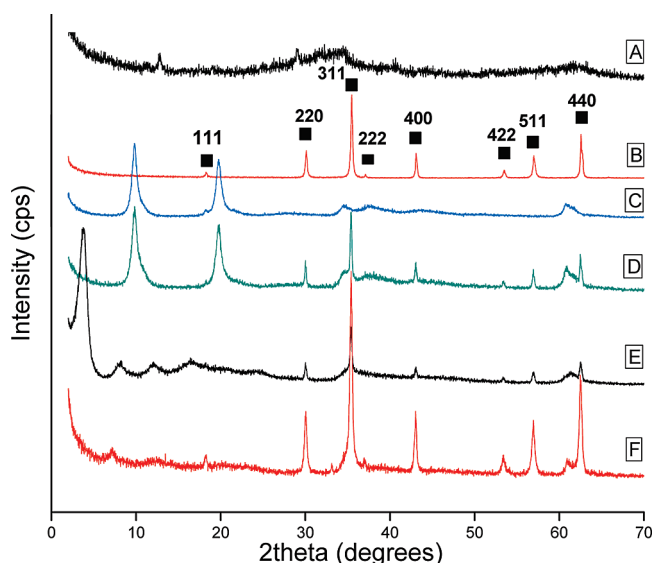


Figure 2. PXRD patterns of (A) CO<sub>3</sub>-LDH, (B) MgFe<sub>2</sub>O<sub>4</sub>, (C) NO<sub>3</sub>-LDH, (D) NO<sub>3</sub>-LDH/MgFe<sub>2</sub>O<sub>4</sub>, (E) IBU-LDH/MgFe<sub>2</sub>O<sub>4</sub>, and (F) GLU-LDH/MgFe<sub>2</sub>O<sub>4</sub>.

Symptomatic treatment for arthritis includes the use of heat, physical therapy, and NSAIDs. Ibuprofen (Figure 1a) is a well-known NSAID, and glucuronic acid (GLU; Figure 1b) is a component of hyaluronan which is also used to treat osteoarthritis of the knee.<sup>31</sup> In this paper, we report new combinations of bioinorganic magnetic core–shell nanocomposites for potential utilization in arthritis therapy. The synthesis and characterization of MgFe<sub>2</sub>O<sub>4</sub>-supported ibuprofen and glucuronic acid intercalated Mg–Al–LDHs with good drug loading capacities and magnetic properties are presented.

## Experimental Section

**Materials.** All chemicals used—Mg(NO<sub>3</sub>)<sub>2</sub>·6H<sub>2</sub>O (Sigma), Fe(NO<sub>3</sub>)<sub>3</sub>·9H<sub>2</sub>O (Sigma), NaOH (Merck), KOH (Merck), Al(NO<sub>3</sub>)<sub>3</sub>·9H<sub>2</sub>O (Carlo Erba), ibuprofen sodium salt (Sigma), and sodium glucuronate monohydrate (Sigma)—were used as received. All other reagents were of analytical grade.

**Synthesis of the Magnetic Core.** A 100 mL solution of Mg(NO<sub>3</sub>)<sub>2</sub>·6H<sub>2</sub>O (0.04 mol) and Fe(NO<sub>3</sub>)<sub>3</sub>·9H<sub>2</sub>O (0.08 mol) and a second solution (220 mL) containing NaOH (0.38 mol) and Na<sub>2</sub>CO<sub>3</sub> (0.32 mol) were simultaneously added into a three-neck flask. The pH was measured as ca. 9. The resulting suspension was stirred for 6 h at 100 °C. The final precipitate, a nonstoichiometric Mg–Fe–CO<sub>3</sub>-LDH (CO<sub>3</sub>-LDH), was separated by centrifugation, washed several times with deionized water, dried at room temperature, and then calcined at 900 °C for 2 h to give the magnetic core material, MgFe<sub>2</sub>O<sub>4</sub>.

**Coating of the Magnetic Core with Mg–Al–NO<sub>3</sub>-LDH Shell.** In order to facilitate the exchange reactions with the

- (12) Khan, A. I.; Lei, L.; Norquist, A. J.; O'Hare, D. *Chem. Commun.* **2001**, 2342–2343.
- (13) Ambrogi, V.; Fardella, G.; Grandolini, G.; Perioli, L.; Tiralti, M. C. *Pharm. Sci. Technol.* **2002**, 3, 1–6.
- (14) Ambrogi, V.; Fardella, G.; Grandolini, G.; Perioli, L. *Int. J. Pharm.* **2001**, 220, 23–32.
- (15) Mohanambe, L.; Vasudevan, S. *J. Phys. Chem. B* **2005**, 109, 15651–15658.
- (16) Gordijo, C. R.; Barbosa, A. S.; Da Costa Ferreira, M.; Constantino, V. R. L.; De Oliveira Silva, D. *J. Pharm. Sci.* **2005**, 94, 1135–1148.
- (17) Costantino, U.; Ambrogi, V.; Nocchetti, M.; Perioli, L. *Microporous Mesoporous Mater.* **2008**, 107, 149–160.
- (18) Del Arco, M.; Cebadera, E.; Gutiérrez, S.; Martín, C.; Montero, M. J.; Rives, V.; Rocha, J.; Sevilla, M. A. *J. Pharm. Sci.* **2004**, 93, 1649–1658.
- (19) Ambrogi, V.; Fardella, G.; Grandolini, G.; Nocchetti, M.; Perioli, L. *J. Pharm. Sci.* **2003**, 92, 1407–1418.
- (20) Del Arco, M.; Fernández, A.; Martín, C.; Rives, V. *Appl. Clay Sci.* **2007**, 36, 133–140.
- (21) Del Arco, M.; Fernández, A.; Martín, C.; Sayalero, M. L.; Rives, V. *Clay Miner.* **2008**, 43, 255–265.
- (22) Del Arco, M.; Fernández, A.; Martín, C.; Rives, V. *Appl. Clay Sci.* **2009**, 42, 538–544.
- (23) Del Arco, M.; Gutiérrez, S.; Martín, C.; Rives, V.; Rocha, J. *J. Solid State Chem.* **2004**, 177, 3954–3962.
- (24) Zhang, H.; Zou, K.; Sun, H.; Duan, X. *J. Solid State Chem.* **2005**, 178, 3485–3493.
- (25) Carja, G.; Chiriac, H.; Lupu, N. *J. Magn. Magn. Mater.* **2007**, 311, 26–30.
- (26) Zhang, H.; Pan, D.; Zou, K.; He, J.; Duan, X. *J. Mater. Chem.* **2009**, 19, 3069–3077.
- (27) Li, F.; Liu, J.; Evans, D. G.; Duan, X. *Chem. Mater.* **2004**, 16, 1597–1602.
- (28) Willey, R. J.; Noirclerc, P.; Busca, G. *Chem. Eng. Commun.* **1993**, 123, 1.
- (29) Poliquen, D.; Chouly C. in: *Arshady, R. Microspheres, Microcapsules and Liposomes. Medical and Biotechnology Applications*; Citus Books: London, 1999; Vol. 2.
- (30) Belikov, V. G.; Kuregyan, A. G. *Pharm. Chem. J-USSR* **2001**, 35, 88–95.

(31) Puhl, W.; Scharf, P. *Ann. Rheum. Dis.* **1997**, 56, 637–640.

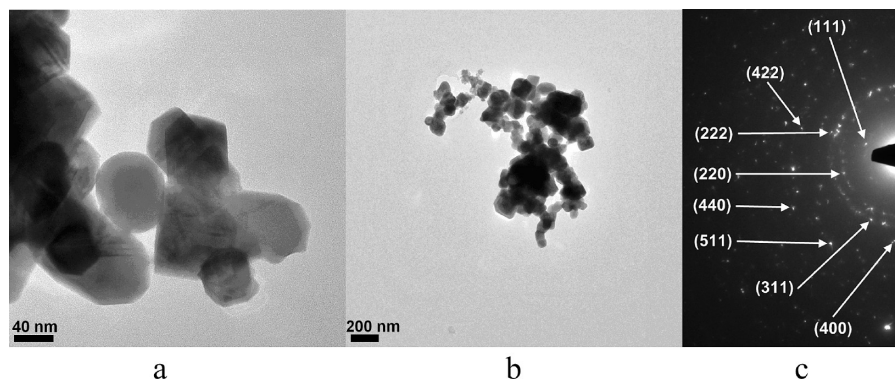


**Figure 3.** TEM bright field images (a, b) and SAED pattern (c) of the magnetic core material.

organic ions, the magnetic core was coated with a LDH containing nitrate instead of carbonate as the interlayer anion. The Mg–Al–NO<sub>3</sub>–LDH (NO<sub>3</sub>–LDH) shell was deposited in situ on the MgFe<sub>2</sub>O<sub>4</sub> magnetic core. A 2 M KOH solution (140 mL) and a suspension (140 mL) containing the metal salts (0.08 mol magnesium nitrate and 0.04 mol aluminum nitrate) and MgFe<sub>2</sub>O<sub>4</sub> (0.80 g) were simultaneously introduced into a three-neck flask by dropwise addition over ca. 1 h under a nitrogen atmosphere. The resulting slurry (pH 9–10) was stirred for 6 h at 70 °C for the deposition of the LDH material on the MgFe<sub>2</sub>O<sub>4</sub> particles and then aged for 24 h at room temperature. During the coating process, the brick-red color of the suspension turned to cedar orange. The final product (NO<sub>3</sub>–LDH/MgFe<sub>2</sub>O<sub>4</sub>) was filtered, washed, and dried at room temperature in a vacuum desiccator. This product was characterized for comparison with the analogous products (AA–LDH/MgFe<sub>2</sub>O<sub>4</sub> where AA = IBU or GLU) containing antiarthritic agents in the interlayer.

**Intercalation of Antiarthritic Agents into LDH Supported on Magnetic Core.** For a comparative evaluation of AA intercalation into LDH, AA–LDH samples were prepared following different methods.

**Direct Synthesis.** A solution (100 mL) containing 0.04 mol of Mg(NO<sub>3</sub>)<sub>3</sub>·6H<sub>2</sub>O and 0.02 mol of Al(NO<sub>3</sub>)<sub>3</sub>·9H<sub>2</sub>O, a second solution (60 mL) of 2 M KOH, and a third solution containing 0.044 mol of ibuprofen sodium salt or sodium glucuronate in 200 mL were slowly added into a MgFe<sub>2</sub>O<sub>4</sub> suspension (0.4 g/30 mL) with vigorous stirring under a nitrogen atmosphere (pH ~9). The system was then refluxed at 70 °C for 6 h under a nitrogen atmosphere. The product (AA–LDH/MgFe<sub>2</sub>O<sub>4</sub>) was filtered, washed thoroughly with water, and then dried at room temperature in a vacuum desiccator.

**Ion Exchange.** The preparation of NO<sub>3</sub>–LDH was as follows: a 100 mL solution containing Mg(NO<sub>3</sub>)<sub>2</sub>·6H<sub>2</sub>O (0.08 mol) and Al(NO<sub>3</sub>)<sub>3</sub>·9H<sub>2</sub>O (0.04 mol) and a base solution (0.42 mol of NaOH/150 mL) were simultaneously added dropwise into a three-neck flask. The slurry (pH ~9) was refluxed under a nitrogen atmosphere at 100 °C for 6 h. A total of 50 mL from the final suspension was withdrawn and added into a 50 mL solution containing 0.044 mol of AA. The pH was adjusted to 9–10 using a 2 M KOH solution, and the resulting slurry was refluxed at 70 °C for 6 h under a nitrogen atmosphere. The product was filtered, washed thoroughly with water, and then dried at room temperature in a vacuum desiccator. This AA–LDH product was then coated on magnesium ferrite. A portion of 0.062 g of AA–LDH was slowly added into a 50 mL suspension containing 0.0325 g of MgFe<sub>2</sub>O<sub>4</sub> with vigorous stirring. The system was then refluxed at 35 °C for 2 h under a nitrogen atmosphere. The product (AA–LDH/MgFe<sub>2</sub>O<sub>4</sub>) was filtered, washed thoroughly with water, and then dried at room temperature in a vacuum desiccator.

**Characterization Studies.** Elemental analysis for metal ions was performed using a Spectro XLAP 2000 PRO XRF X-ray fluorescence spectrometer, while for carbon and hydrogen it was performed on an Elementar Analysensysteme GmbH varioMICRO CHNS. The water content was determined by thermogravimetry. Powder X-ray diffraction patterns (PXRD) were recorded using a Rigaku D/MAX-2200 diffractometer equipped with graphite-filtered Cu K $\alpha$  radiation ( $\lambda$  = 1.54056 Å) from 3 to 70° (2 $\theta$ ) at a scanning rate of 4° min<sup>-1</sup>. Fourier transform infrared spectra (FTIR) were recorded in the range 4000–400 cm<sup>-1</sup> on a Perkin-Elmer Spectrum One using the KBr pellet technique. Simultaneous thermogravimetric and differential thermal analyses (TGA-DTA) were carried out in nitrogen on a Shimadzu DTG-60H thermal analysis system at a heating rate of 10 °C/min. The morphology and dimension of the synthesized products were observed with an FEI quanta 200 FEG scanning electron microscope (SEM). Transmission electron microscopy (TEM) and selected area electron diffraction (SAED) were performed using an FEI Tecnica G2 F30 instrument operating at 300 or 100 kV. Magnetism of the products was measured at room temperature with a vibrating sample magnetometer (Quantum Designed Physical Property Measurement System) in a magnetic field range of  $\pm$ 30 kOe.

## Results and Discussion

**Synthesis of the Magnetic Core.** The magnetic core material was obtained by calcination of an iron-containing nonstoichiometric LDH with interlayer carbonate ions. CO<sub>3</sub>–LDH was synthesized by the coprecipitation technique with a Mg/Fe molar ratio of 1:2. Usually, the M<sup>II</sup>/M<sup>III</sup> molar ratio should be at least equal to 2 to obtain pure LDHs with the hydrotalcite-like structure. Incorporation of excess Fe<sup>3+</sup> ions into the solid resulted in the formation of a nonstoichiometric, mostly amorphous LDH, but affording stoichiometric, crystalline magnesium ferrite spinel upon calcination. Figure 2 illustrates the PXRD patterns of the CO<sub>3</sub>–LDH precursor (A) and its calcination product (B). Upon calcination of the precursor LDH, characteristic sharp reflections (indicative of good crystallinity) of MgFe<sub>2</sub>O<sub>4</sub> (JCPDS 17–465) at 18.3° (111), 30.1° (220), 35.5° (311), 36.9° (222), 43.1° (400), 53.5° (422), 57.0° (511), and 62.6° (440) were observed, Figure 2B. No other crystalline phases were detected.

The detailed morphology of the magnesium ferrite core was investigated by TEM. The TEM bright field image shown in Figure 3a indicates that nanosized MgFe<sub>2</sub>O<sub>4</sub> crystallites are polyhedral and mostly in the 50–80 nm size range. The crystallites tend to agglomerate as chainlike



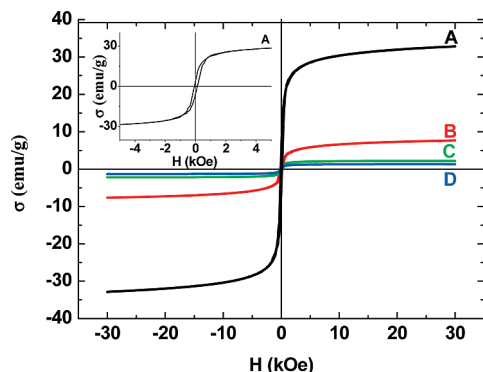


**Figure 4.** Room-temperature magnetizations of (A)  $\text{MgFe}_2\text{O}_4$ , (B)  $\text{NO}_3\text{-LDH/MgFe}_2\text{O}_4$ , (C)  $\text{GLU-LDH/MgFe}_2\text{O}_4$ , and (D)  $\text{IBU-LDH/MgFe}_2\text{O}_4$  (the inset displays the enlarged central portion of the hysteresis curve A).

clusters (Figure 3b). The corresponding SAED pattern, displayed in Figure 3c, clearly highlights the diffraction nature of  $\text{MgFe}_2\text{O}_4$ . The spotty diffraction rings (111), (220), (311), (222), (400), (422), (511), and (440) agree with the PXRD pattern (B) shown in Figure 2 and with the standard data (JCPDS 17–465). No diffraction spots corresponding to those of  $\text{MgO}$  (JCPDS 77–2179) or to other secondary phases were observed.

Room temperature magnetic characteristics of the core material were investigated by recording the magnetization versus applied field curve (Figure 4). The observed minimal hysteresis behavior (inset in Figure 4) and saturation magnetization value,  $\sigma_s = 29.6$  emu/g, indicate extremely soft ferromagnetism.<sup>32</sup> The  $\sigma_s$  value obtained concurs with the reported values for spinel ferrites prepared by calcination of LDHs.<sup>27,24,33</sup>

**Coating of the Magnetic Core with Mg–Al– $\text{NO}_3$ –LDH Shell.** As described in the Experimental Section, the  $\text{NO}_3\text{-LDH}$  shell was in situ deposited on the magnetic core in an aqueous  $\text{MgFe}_2\text{O}_4$  suspension. Cedar-orange colored, monodisperse  $\text{NO}_3\text{-LDH/MgFe}_2\text{O}_4$  particles were obtained, and all of the following analytical data were collected on samples from the same batch. The PXRD pattern of this product (pattern D) included in Figure 2 shows diffraction maxima corresponding to the  $\text{NO}_3\text{-LDH}$  shell (pattern C) and also to magnesium ferrite (pattern B). The two intense peaks at low  $2\theta$  angles,  $9.9^\circ$  and  $19.8^\circ$ , are due to  $d_{003}$  and  $d_{006}$  reflections that are characteristic for LDHs with interlayer nitrate ions. From the spacing for the  $d_{003}$  reflection, the interlayer distance was calculated as 9.00 Å. The gallery height was found as 4.2 Å by subtracting the layer thickness (4.8 Å)<sup>34</sup> from the basal spacing. These values are appropriate for a tilted intercalation of nitrate ions between the LDH layers.<sup>6</sup>

The FTIR spectra of the samples  $\text{NO}_3\text{-LDH}$ ,  $\text{MgFe}_2\text{O}_4$ , and  $\text{NO}_3\text{-LDH/MgFe}_2\text{O}_4$  are included in Figure 5A–C. The strong and broad bands centered around  $3450\text{ cm}^{-1}$  in A and C are associated with the O–H stretching vibrations of the hydroxyl groups in the brucite layers and interlayer water molecules. The water

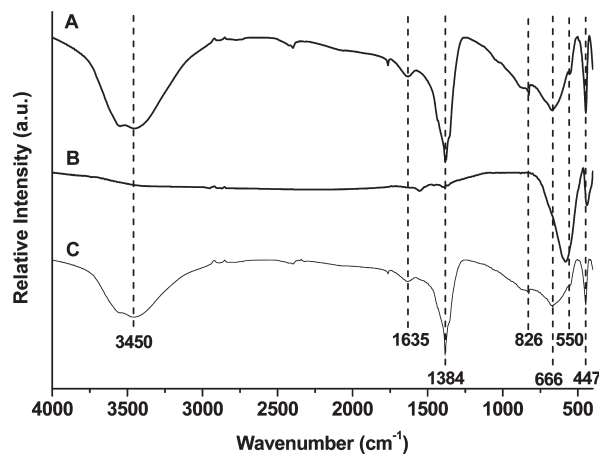


**Figure 5.** FTIR spectra of (A)  $\text{NO}_3\text{-LDH}$ , (B)  $\text{MgFe}_2\text{O}_4$ , and (C)  $\text{NO}_3\text{-LDH/MgFe}_2\text{O}_4$ .

deformation band is observed at  $1635\text{ cm}^{-1}$ . Peaks corresponding to the  $\nu_3$  and  $\nu_2$  modes of interlayer nitrate ions appear respectively at  $1384\text{ cm}^{-1}$  and  $826\text{ cm}^{-1}$ . The shoulder at  $550\text{ cm}^{-1}$  and the sharp peak at  $447\text{ cm}^{-1}$  are assigned to metal–oxygen lattice vibrations and the broad band at  $666\text{ cm}^{-1}$  to M–O–H bending.<sup>35,36</sup> The sharp peak at  $447\text{ cm}^{-1}$  is diagnostic for lattice ordering and is characteristic of well-ordered  $\text{Mg}_2\text{-Al-LDHs}$ .<sup>37</sup> The hydroxyl and nitrate peaks disappear in the spectrum of the calcined product (B), and instead new bands appear at  $\nu_1 = 570\text{ cm}^{-1}$  and  $\nu_2 = 439\text{ cm}^{-1}$  indicative of nano-sized magnesium ferrite spinel formation.<sup>38</sup> The spectrum of the LDH-coated magnesium ferrite (C) displays peaks due to the LDH and  $\text{MgFe}_2\text{O}_4$  components where the  $\nu_1$  and  $\nu_2$  bands of the spinel should have been possibly overlapped by the M–O peaks of the LDH.

Figure 6a shows the SEM photograph of  $\text{NO}_3\text{-LDH}$  where the layered structure can be visualized. Figure 6b represents the image of  $\text{NO}_3\text{-LDH}$  after being coated on magnesium ferrite. The sample consists of roughly spherical particles with sizes in the range of 50–150 nm. There is no unwrapped core or separate irregular particles in the SEM image, which indicates the homogeneous distribution of two phases. A detailed examination of the image reveals that the spheres with an average diameter around 100 nm are covered by a LDH shell of 20–40 nm thickness. A typical TEM image (Figure 6c) clearly demonstrates the core–shell nature of the spheres where the black rigid  $\text{MgFe}_2\text{O}_4$  particles are dispersed in the gray matrix of the LDH. The SAED pattern (Figure 6d) includes spots referring to  $\text{MgFe}_2\text{O}_4$  and LDH reflections, thus confirming the presence of both phases in the composite material. The high-resolution (HR)TEM image shown in Figure 6e exhibits equally spaced lattice rows of the dense ferrite core surrounded by a less dense material.

The saturation magnetization value of the  $\text{NO}_3\text{-LDH/MgFe}_2\text{O}_4$  sample was found (Figure 4B) to be much

(32) Jiles, D. C. *Introduction to Magnetism and Magnetic Materials*, 2nd ed.; Chapman & Hall: New York, 1998.

(33) Liu, J.; Li, F.; Evans, D. G.; Duan, X. *Chem. Commun.* **2003**, 542–543.

(34) Whilton, N. T.; Vickers, P. J.; Mann, S. J. *Mater. Chem.* **1997**, 7, 1623–1629.

(35) Hernandez-Moreno, M. J.; Ulbarri, M. A.; Rendon, J. L.; Serna, C. J. *Phys. Chem. Miner.* **1985**, 12, 34–38.

(36) Xu, Z. P.; Zeng, H. C. *J. Phys. Chem. B* **2001**, 105, 1743–1749.

(37) Richardson, M. C.; Braterman, P. S. *J. Phys. Chem. C* **2007**, 111, 4209–4215.

(38) Pradeep, A.; Priyadharsini, P.; Chandrasekaran, G. *J. Magn. Magn. Mater.* **2008**, 320, 2774–2779.

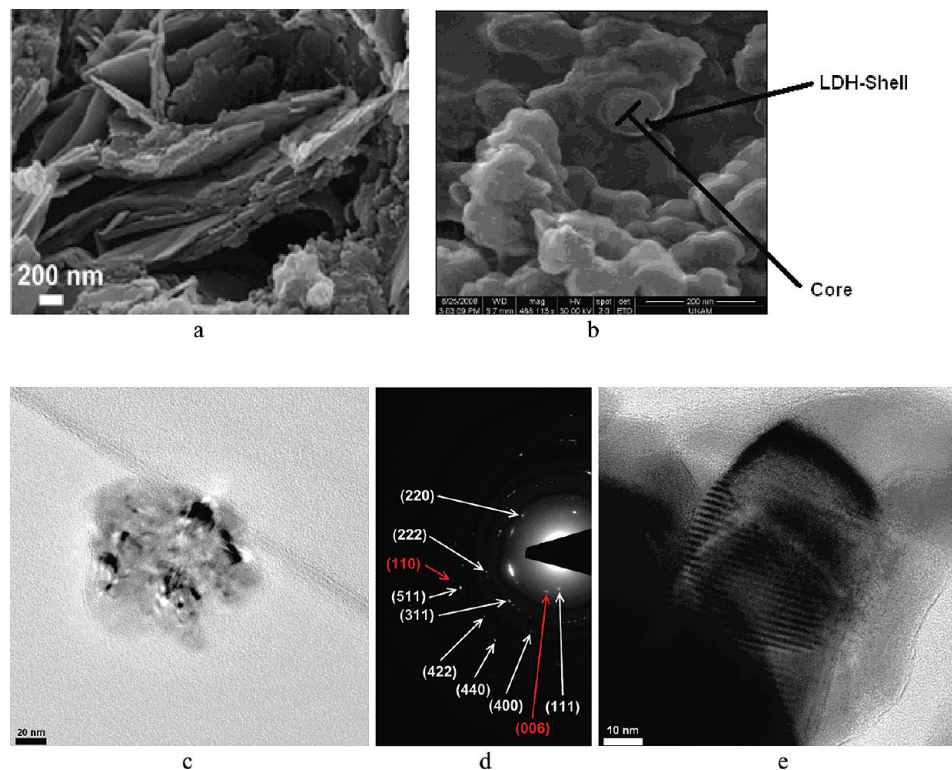


**Figure 6.** (a) SEM image of  $\text{NO}_3$ -LDH and (b) SEM image, (c) TEM image, (d) SAED pattern (white arrows,  $\text{MgFe}_2\text{O}_4$ ; red arrows, LDH), and (e) HRTEM image of  $\text{NO}_3$ -LDH/ $\text{MgFe}_2\text{O}_4$ .

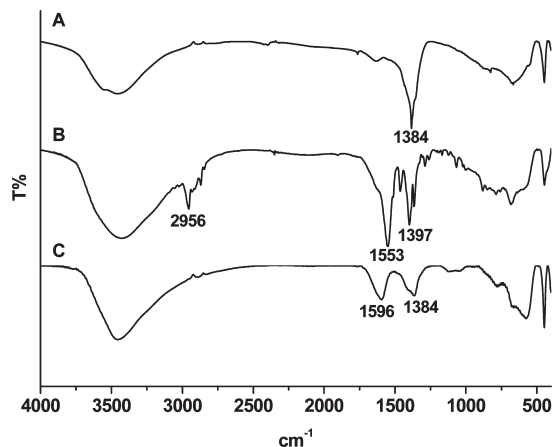


**Figure 7.** FTIR spectra of (A)  $\text{NO}_3$ -LDH/ $\text{MgFe}_2\text{O}_4$ , (B) IBU-LDH/ $\text{MgFe}_2\text{O}_4$ , and (C) GLU-LDH/ $\text{MgFe}_2\text{O}_4$ .

lower ( $\sigma_s$  2.19 emu/g) than that of the  $\text{MgFe}_2\text{O}_4$  core ( $\sigma_s$  29.6 emu/g). This change is reasonable on the basis of the core-shell structure of the sample where the ferromagnetic core is covered by a nonmagnetic shell and the molar fraction of the magnetic core is lower than in bulk ferrite. Nevertheless, the hysteresis behavior was still noticeable, and the measured magnetization value makes the  $\text{NO}_3$ -LDH/ $\text{MgFe}_2\text{O}_4$  system usable for suitable magnetic applications.

**Intercalation of Ibuprofen and Glucuronate Anions into  $\text{NO}_3$ -LDH Supported on Magnetic Core.** Intercalation of antiarthritic agents into  $\text{NO}_3$ -LDH/ $\text{MgFe}_2\text{O}_4$  was successful both by direct synthesis and by ion exchange methods, but the latter gave more satisfactory results. The products obtained by direct synthesis showed feature,

broad XRD peaks indicative of purely developed crystallinity due to the layer stacking defects caused by simultaneous deposition of the LDH shells onto the magnetic core and the self-organization of the large AA anions in the interlayer space. The intercalation experiments were therefore continued with the ion-exchange method conducted under a nitrogen atmosphere to avoid carbonate intercalation from atmospheric carbon dioxide. The complete removal of nitrate ions during the ion-exchange process was evidenced by the FTIR spectra. The characteristic nitrate peak at  $1384\text{ cm}^{-1}$  in the spectrum of the precursor LDH compound (Figure 7A) disappeared in the spectra of the products, and new peaks corresponding to the organic intercalates appeared instead in addition to the existing major bands due to the inorganic network (as discussed for Figure 5 in the previous paragraphs). Figure 7B displays the spectrum of IBU-LDH/ $\text{MgFe}_2\text{O}_4$ , where the characteristic vibrations of the alkyl chain ( $2956\text{ cm}^{-1}$ ) and antisymmetric and symmetric vibrations of the carboxylate group ( $1553\text{ cm}^{-1}$  and  $1397\text{ cm}^{-1}$ , respectively) of intercalated ibuprofen anions are seen. Likewise, the characteristic  $\nu_a(\text{COO})$  and  $\nu_s(\text{COO})$  vibrations of intercalated glucuronate anions can be seen at  $1596\text{ cm}^{-1}$  and  $1384\text{ cm}^{-1}$ , respectively, in Figure 7C. The bands of the intercalants were found to be similar with respect to their positions to those in the spectra of their corresponding pure salts but broader due to different interactions with the LDH matrix.

Figure 2E and F show the PXRD patterns of the samples obtained by the ion-exchange treatment for both drugs. The patterns consist of sharp reflections at  $2\theta = 30.2^\circ, 35.5^\circ, 37.1^\circ, 43^\circ, 53.5^\circ, 57^\circ$ , and  $62.6^\circ$  corresponding to the  $\text{MgFe}_2\text{O}_4$  spinel and also other reflections at

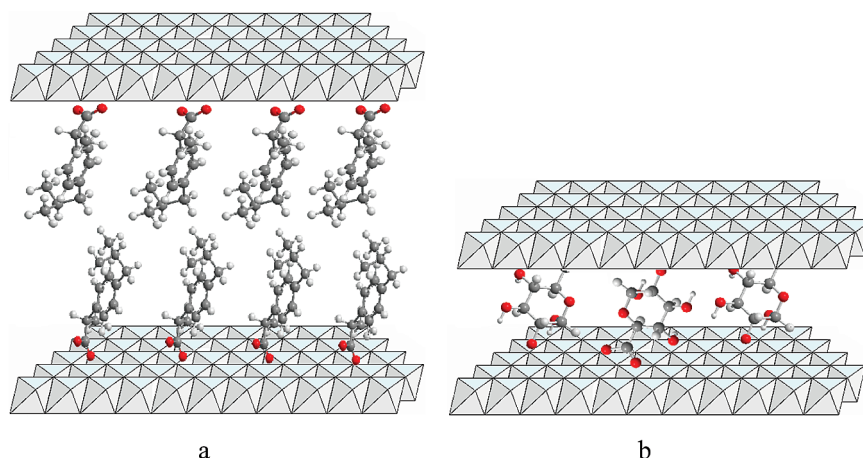


**Figure 8.** Suggested arrangements of (a) ibuprofen and (b) glucuronate anions in LDH galleries.

lower  $2\theta$  values corresponding to LDH. Owing to the incorporation of larger organic anions, the basal spacing of LDH increased from 9.00 Å (nitrate form) to 22.87 Å with ibuprofen and to 12.52 Å with glucuronate. Because the layers are about 4.8-Å-thick, the gallery heights were respectively enlarged to 18.07 and 7.72 Å. The observed basal spacings can be explained by a vertical orientation of the organic anions considering the dimensions and the shapes of the organic intercalants. The molecular dimensions of the ibuprofen molecule (length, 10.3 Å; width, 5.2 Å; and thickness, 3.4 Å) were estimated by Messtre et al., with Gaussian 03 employing the semiempirical PM3 method.<sup>39</sup> The interlayer space of about 18 Å is much larger (almost twice) than the long axis of the ibuprofen anion (10.3 Å), and thus a slightly tilted bilayer arrangement is expected, where the carboxylate groups are pointing to the hydroxide layers, as proposed in Figure 8a and as indicated by spectroscopic and simulation studies reported by Mohanambe and Vasudevan.<sup>15</sup> On the other hand, a tilted interdigitated arrangement of glucuronate anions appears to be plausible, assuming their dimensions are identical to those in the crystalline state.<sup>40</sup> The intercalated glucuronate anions about 7 Å in length would interact with the positive hydroxide layers through their carboxylate groups and through hydrogen bonds and also with each other such that the carboxylate group of each anion is hydrogen-bonded to the tail groups of the neighbors.

The structural stability of the compounds was examined by thermogravimetry. Thermal decompositions of  $\text{NO}_3\text{-LDH/MgFe}_2\text{O}_4$  and  $\text{AA-LDH/MgFe}_2\text{O}_4$  samples generally proceeded through the steps of (i) desorption of the physically adsorbed water, (ii) removal of the interlayer water, and (iii) dehydroxylation of the layers and decomposition of the interlayer anions. The temperature interval for these steps started from room temperature up to ca. 500 °C for both  $\text{NO}_3\text{-LDH/MgFe}_2\text{O}_4$  and  $\text{IBU-LDH/MgFe}_2\text{O}_4$ , while it was gently extended to higher temperatures for  $\text{GLU-LDH/MgFe}_2\text{O}_4$  (Figure 9). The increase in the stability of the  $\text{GLU-LDH}$  structure results from the increased interlayer attractions

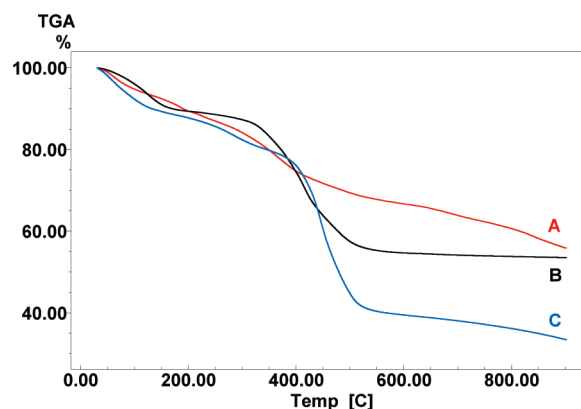


**Figure 9.** TGA curves for (A)  $\text{GLU-LDH/MgFe}_2\text{O}_4$ , (B)  $\text{NO}_3\text{-LDH/MgFe}_2\text{O}_4$ , and (C)  $\text{IBU-LDH/MgFe}_2\text{O}_4$ .

due to effective hydrogen bonding through bridging glucuronate anions which possess several hydrogen bonding donor/acceptor sites available to interact with the layers (Figure 1). The decomposition temperatures of the intercalated organic anions also shifted to higher values. Degradation of the intercalated ions started at ca. 400 °C and proceeded rapidly for ibuprofen and slowly for glucuronate. Considering that pure ibuprofen and glucuronate salts decompose around 250 °C,<sup>41,42</sup> it implies that the thermal stabilities of these agents were significantly enhanced after intercalation.

Together with the elemental chemical analysis data, thermogravimetric weight loss values were used to determine the composition of the prepared samples (Table 1). The molar  $\text{Mg/Al}$  ratios ( $2.0 \pm 0.2$ ) were found to be close to the ratio existing in the starting solutions. The C, H, N elemental analysis results are in good agreement with the proposed compositions. A minor amount of N was found in the  $\text{GLU-LDH}$  sample, suggesting that, in addition to  $\text{GLU}$  anions, some nitrate ions are also present in the interlayer region, but their presence in the FTIR spectrum was possibly masked by the  $\nu_s(\text{COO})$  vibrations of intercalated glucuronate anions at  $1384\text{ cm}^{-1}$  (Figure 7B). The weight loss values up to 150 °C are consistent with the

(39) Messtre, A. S.; Pires, J.; Nogueira, J. M. F.; Carvalho, A. P. *Carbon* 2007, 45, 1979–1988.

(40) Gurr, G. E. *Acta Crystallogr.* 1963, 16, 690–696.

(41) Ribeiro, Y. A.; de Oliveira, S.; Leles, M. I. G.; Juiz, S. A.; Ionashimo, M. J. *Therm. Anal.* 1996, 46, 1645–1655.

(42) Perlin, A. S. *Can. J. Chem.* 1952, 30, 278–290.



**Table 1.** Proposed Chemical Compositions of the Samples with Some Analytical Data<sup>a</sup>

sample	composition	C (%)	H (%)	N (%)	H <sub>2</sub> O (%) <sup>b</sup>	total weight loss (%) <sup>c</sup>
NO <sub>3</sub> -LDH	7{Mg <sub>0.66</sub> Al <sub>0.34</sub> (OH) <sub>2</sub> (NO <sub>3</sub> ) <sub>0.34</sub> ·0.7H <sub>2</sub> O}·MgFe <sub>2</sub> O <sub>4</sub>		2.94 (2.79)	3.96 (3.91)	9.2 (10)	46 (43)
IBU-LDH	10{Mg <sub>0.64</sub> Al <sub>0.36</sub> (OH) <sub>2</sub> (IBU) <sub>0.36</sub> ·0.7H <sub>2</sub> O}·MgFe <sub>2</sub> O <sub>4</sub>	34.6 (33.9)	5.83 (5.96)		9.7 (8.7)	66 (63)
GLU-LDH	3{Mg <sub>0.66</sub> Al <sub>0.34</sub> (OH) <sub>2</sub> (NO <sub>3</sub> ) <sub>0.09</sub> (GLU) <sub>0.25</sub> ·0.7H <sub>2</sub> O}·MgFe <sub>2</sub> O <sub>4</sub>	8.77 (9.36)	3.68 (3.07)	0.68 (0.65)	6.5 (6.5)	44 (43)

<sup>a</sup> Values in parentheses refer to calculated values. <sup>b</sup> Thermogravimetric mass loss up to 130 °C. <sup>c</sup> Calculated on the basis of the residues: 5.5MgO·Al<sub>2</sub>O<sub>3</sub>·Fe<sub>2</sub>O<sub>3</sub> for NO<sub>3</sub>-LDH, 7.5MgO·1.5Al<sub>2</sub>O<sub>3</sub>·Fe<sub>2</sub>O<sub>3</sub> for IBU-LDH, and 3MgO·0.5Al<sub>2</sub>O<sub>3</sub>·Fe<sub>2</sub>O<sub>3</sub> for GLU-LDH.

**Table 2.** Some Characteristics of MgFe<sub>2</sub>O<sub>4</sub> and LDH/MgFe<sub>2</sub>O<sub>4</sub> Samples

sample	<i>d</i> <sub>003(LDH)</sub> (Å)	AA <sup>a</sup>	MgFe <sub>2</sub> O <sub>4</sub> <sup>a</sup>	σ <sub>s</sub> (emu/g)
MgFe <sub>2</sub> O <sub>4</sub>			100	29.6
NO <sub>3</sub> -LDH/MgFe <sub>2</sub> O <sub>4</sub>	9.0		23.5	2.19
IBU-LDH/MgFe <sub>2</sub> O <sub>4</sub>	22.87	45	12	1.31
GLU-LDH/MgFe <sub>2</sub> O <sub>4</sub>	12.52	25	35	7.65

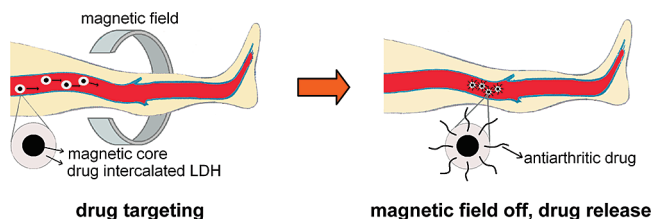
<sup>a</sup> Weight percentage.

proposed water content. The recorded total mass losses were respectively 46%, 66%, and 44% for NO<sub>3</sub>-LDH/MgFe<sub>2</sub>O<sub>4</sub>, IBU-LDH/MgFe<sub>2</sub>O<sub>4</sub>, and GLU-LDH/MgFe<sub>2</sub>O<sub>4</sub>. In all cases, the LDH structures start to collapse around 500 °C and are expected to give MgAl<sub>2</sub>O<sub>4</sub> and MgO mixed with MgFe<sub>2</sub>O<sub>4</sub> as the final decomposition end products.<sup>43,44</sup> The observed total weight loss values are in reasonable agreement with the values calculated by assuming that the residual material is composed of *x*MgO + *y*Al<sub>2</sub>O<sub>3</sub> + *z*Fe<sub>2</sub>O<sub>3</sub> where *x*, *y*, and *z* refer to the stoichiometric numbers of the corresponding metals in the proposed formulas (Table 1, footnote). The total IBU and GLU contents were respectively calculated as 45% and 25% on the basis of the compositions given in Table 1.

Some characteristic properties of the products are summarized in Table 2. The observed saturation magnetization values are related to the amount of the magnetic core in the composites. The σ<sub>s</sub> values of the AA-LDH/MgFe<sub>2</sub>O<sub>4</sub> samples were found to be much lower than that of the pure ferrite spinel because of the presence of the nonmagnetic LDH shell containing intercalated organic anions. The decrease in the σ<sub>s</sub> value was more significant with ibuprofen. In parallel to the expansion of the LDH galleries and incorporation of a high amount of ibuprofen anions, the nonmagnetic contribution reduces the σ<sub>s</sub> value to 1.31 emu/g (Table 2).

## Summary and Conclusions

In this work, magnetic nanocomposites carrying antiarthritic agents were successfully prepared from

**Scheme 1.** A Schematic Description of Magnetic Arthritis Therapy with Drug Intercalated LDHs Supported on a Magnesium Ferrite Core

LDHs. An iron-containing LDH material was used as the precursor to the magnetic core; its calcination yielded nanosized MgFe<sub>2</sub>O<sub>4</sub> crystallites, which showed soft ferromagnetism at room temperature. Magnetic particles were then coated with a LDH containing interlayer nitrate ions. The exchange of nitrate ions with the ibuprofen and glucuronate anions yielded drug-carrying magnetic LDHs. TEM analyses revealed that the products adopt a core-shell structure. On intercalating the AA agents, the layers of the LDH were expanded. Maximum expansion has been noted with ibuprofen. The strong electrostatic interactions between the LDH layers and the guest anions have led to a high content of intercalated AA agents; drug-carrying LDH/MgFe<sub>2</sub>O<sub>4</sub> structures were found to contain 45% ibuprofen and 25% glucuronate. TG measurements revealed that the thermal stabilities of the intercalated agents are significantly enhanced. The LDH/MgFe<sub>2</sub>O<sub>4</sub> system thus appears to be a safe and nontoxic drug delivery system along with good intercalating properties for protecting drugs against chemical or enzymatic degradation. The potential of using this system in magnetic targeted delivery (magnetic-field-controlled delivery of a drug to the targeted organ and the subsequent release, Scheme 1) is of great promise.

**Acknowledgment.** This work was financially supported by the Turkish Scientific and Technological Research Council (project: 107T034). The authors wish to thank Mr. Deniz Konuk for providing assistance in the preparative studies. V.R. thanks financial support from MICINN (grant MAT2009-08526) and ERDF.

(43) Cheng, S.; Lin, J.-T. In *Expanded Clays and Microporous Solids*; Ocelli, M. L., Robson, H. E., Eds.; Van Nostrand Reinhold: New York, 1992.

(44) Li, L.; Ma, S.; Liu, X.; Yue, Y.; Hui, J.; Xu, R.; Bao, Y.; Rocha, J. *Chem. Mater.* **1996**, *8*, 204–208.